Detecting dark domain walls through their impact on particle trajectories in tailored ultrahigh vacuum environments

Kate Clements,[1,*] Benjamin Elder,[2,†] Lucia Hackermueller,[1,‡] Mark Fromhold,[1,§] and Clare Burrage[1,‖]
[1]School of Physics and Astronomy, University of Nottingham, Nottingham NG7 2RD, United Kingdom
[2]Department of Physics and Astronomy, University of Hawai'i, 2505 Correa Road, Honolulu, Hawaii 96822, USA

(Received 11 August 2023; revised 27 November 2023; accepted 1 May 2024; published 14 June 2024)

Light scalar fields, with double well potentials and direct matter couplings, undergo density driven phase transitions, leading to the formation of domain walls. Such theories could explain dark energy or dark matter or source the nanohertz gravitational-wave background. We describe an experiment that could be used to detect such domain walls in a laboratory environment, solving for the scalar field profile and showing how the domain wall affects the motion of a test particle. We find that, in currently unconstrained regions of parameter space, the domain walls leave detectable signatures.

DOI: 10.1103/PhysRevD.109.123023

I. INTRODUCTION

Light scalar fields are commonly invoked to solve cosmological mysteries, including the nature of dark matter [1,2], the source of the current accelerating expansion of the Universe [3,4], or whether gravity is modified on the largest cosmological scales [5]. Such scalar fields can arise in string theory [6,7], and can be introduced into low-energy effective field theory descriptions of physics in natural ways [8–13].

Adding a scalar field to the Standard Model Lagrangian can result in a wide range of phenomenology depending on the choice of potential and couplings. Allowing scalar potentials beyond just a simple mass term can weaken experimental constraints due to screening [4,14,15], but also yield novel detectable signatures. In this work we focus on scalar fields that couple to matter and have a symmetry breaking potential, sometimes referred to as symmetron models, which allows for the formation of domain wall topological defects when the local energy density is lowered below a critical threshold [16,17] (for related work see Refs. [18–23]).

Domain walls are planar topological defects that store energy and form after the scalar field goes through a phase transition. There has been much study of the observable consequences of scalar fields undergoing temperature driven phase transitions in the early Universe [24,25]. Here, we focus on an alternative possibility that, due to direct couplings to matter, the phase transitions are driven by changes in energy density, leading to detectable effects in laboratory experiments [15]. The coupling to matter changes the scaling of a cosmological network of domain walls [26,27], and they may be unstable on cosmological timescales [28]. We call these "dark" domain walls, because the coupling of the scalar field to matter will be difficult to see unless experiments and observables are carefully tailored.

A direct coupling of the scalar field to matter implies the following: (1) The scalar field mediates a fifth force, whose strength is proportional to the background value of the scalar. (2) Symmetry breaking is controlled by the local matter density. (3) Once formed, the domain walls can be "pinned" to matter structures. Consequently, matter particles passing through a domain wall can be trapped or deflected [26,29]. The possibility of detecting topological defects through these effects has been considered in Ref. [30] in the context of experiments with ultracold neutrons. On a different scale, a dark domain wall could explain the planes of satellite galaxies around the Milky Way and Andromeda [29] or make cosmic voids emptier [31]. A network of cosmological domain walls has also been proposed as a source for the nanohertz stochastic background of gravitational waves [32–35].

In this work we explore the conditions needed for domain walls to form inside a laboratory vacuum chamber and the implications for the matter structures needed to pin the domain

*Kate.Clements@nottingham.ac.uk
†bcelder@hawaii.edu
‡Lucia.Hackermuller@nottingham.ac.uk
§Mark.Fromhold@nottingham.ac.uk
‖Clare.Burrage@nottingham.ac.uk

walls in place. We show that the Kibble-Zurek mechanism alone is not sufficient to facilitate the formation of domain walls as the gas density changes inside a vacuum chamber, but that their formation can be encouraged with a suitable designed experiment. We demonstrate that there exists a region of currently unconstrained parameter space, within which such domain walls could cause measurable deflections of clouds of cold atoms. We work with a $(-,+,+,+)$ metric and use natural units unless otherwise stated.

II. THE MODEL

We consider a scalar field theory of the form

$$S = \int \mathrm{d}^4x\sqrt{-g}\left[\frac{R}{16\pi G} - \frac{1}{2}\nabla_\mu\phi\nabla^\mu\phi + \frac{1}{2}\mu^2\phi^2 - \frac{\lambda}{4}\phi^4\right] + S_\mathrm{m}[\tilde{g}_{\mu\nu}, \psi_i], \tag{1}$$

where the scalar field is conformally coupled to matter fields ψ_i through the metric $\tilde{g}_{\mu\nu} = (1+\frac{\phi^2}{2M^2})^2 g_{\mu\nu}$ and the matter action is S_m. Parameters μ and M are constant mass scales, and λ is a positive dimensionless constant. A test particle experiences a nonrelativistic fifth force mediated by the scalar field

$$\mathbf{F}_5 = -\nabla\left(1+\frac{\phi^2}{2M^2}\right) \approx -\frac{\phi\nabla\phi}{M^2}. \tag{2}$$

In the presence of nonrelativistic matter, with energy density ρ, the behavior of the scalar field is governed by a density-dependent effective potential,

$$V_\mathrm{eff}(\phi) = -\frac{1}{2}\mu^2\left(1-\frac{\rho}{\mu^2M^2}\right)\phi^2 + \frac{\lambda}{4}\phi^4. \tag{3}$$

The coefficient of the quadratic term is positive or negative depending on whether the density is above or below the critical density, $\rho_\star \equiv \mu^2M^2$.

Different choices of the model parameters explain different observed phenomena. When $\rho_\star$ coincides with the present cosmological density, it may help explain dark energy [16,17]. When $\mu M_\mathrm{pl} = \sqrt{\lambda}M^2$, the fifth force in vacuum is of gravitational strength, suggesting a connection to theories of modified gravity. When $\mu \approx 10^{-27}$ eV and $\sqrt{\lambda}M \approx 10^{-24}$ eV, the model can explain the observed planes of Milky Way satellite galaxies [29]. When $\mu/\lambda^{1/3} \approx$ MeV, domain walls can make up a fraction of the dark matter density in the Universe today [36]. When $\mu/\lambda^{1/3} \approx 10^5$ GeV, the domain walls could source the observed stochastic gravitational-wave background [34]. When $\mu = 2.4$ meV $\sim 1/(8.2\times10^{-5}$ m), the one-loop Coleman-Weinberg correction to the scalar potential is $\Delta V \approx \mu^4$, which at this value of μ matches the cosmological constant of the Universe [37,38]. The motivated parameter space is therefore extremely large, and the range of interesting values of λ stretches from $\lambda \sim \mathcal{O}(1)$ to, e.g., $\lambda \sim 10^{-94}$ for a theory with $M \sim M_\mathrm{pl}$, $\mu \sim 1/$Mpc and a fifth force of gravitational strength. We will see that experiments of the type we propose in this work become more sensitive to the presence of domain walls for smaller values of λ and also that for very small values of λ the experiment would be able to probe dark matter or early Universe physics. However, we acknowledge that such small values of λ may be considered fine-tuned or unnatural.

For $\lambda = 10^{-10}$ and $\lambda = 10^{-30}$, current constraints on the model parameters are shown by the dark opaque shaded region in Figs. 1 and 2. The white solid line in Fig. 1 indicates where the fifth force has gravitational strength in vacuum and the white dotted line in Fig. 2 indicates where the domain walls could make up part of dark matter. The parameter space shown in these figures corresponds to critical densities from $\rho_\star \sim 10^{-14}$ to 10^{11} g/cm^3. We note

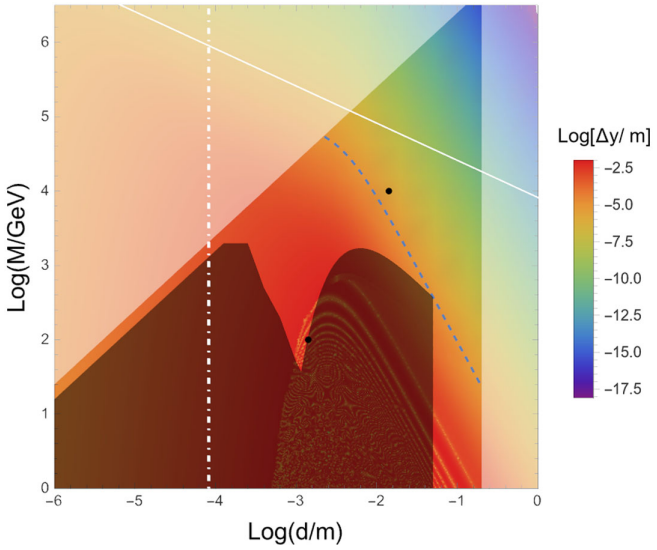

FIG. 1. Model parameter space when $\lambda = 10^{-10}$. The dark opaque shaded region is excluded by existing constraints from neutron bouncing experiments, cold neutron interferometry [39], and atom interferometry [40]. The light opaque shaded regions show where domain walls would not form within our idealized vacuum chamber. The color scale shows the expected deviation from linear motion of a test particle, $\Delta y = y(t) - y_0 + \dot{y}_0 t$, after 10 s with initial velocity $\dot{y}_0 = 10^{-3}$ m/s, and starting position $y_0 = 5\times10^{-3}$ m moving perpendicularly to an infinite straight domain wall located at $y = 0$. Curved colored regions indicate the oscillations caused by the test particle being trapped by the domain wall. The dashed blue line shows where $\Delta y \approx 10$ μm, indicating the limit of current detectability. The white solid line shows where the fifth force in vacuum has gravitational strength; $\mu M_\mathrm{pl} = \sqrt{\lambda}M^2$. The white dash-dotted line corresponds to $d = 8.2\times10^{-5}$ m where quantum corrections from the scalar field could play the role of the cosmological constant [37,38]. Two black dots show the example points in parameter space discussed in Sec. IV B.

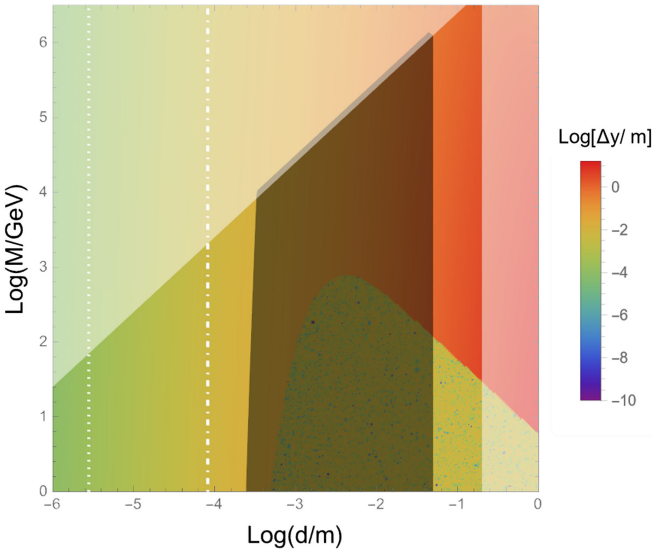

FIG. 2. Model parameter space when $\lambda = 10^{-30}$. The dark opaque shaded region is excluded by existing constraints from atom interferometry [40]. The light opaque shaded regions show where domain walls would not form within our idealized vacuum chamber. The color scale shows the expected deviation from linear motion of a test particle, $\Delta y = y(t) - y_0 + \dot{y}_0 t$, after 10 s with initial velocity $\dot{y}_0 = 10^{-3}$ m/s, and starting position $y_0 = 5 \times 10^{-3}$ m moving perpendicularly to an infinite straight domain wall located at $y = 0$. The curved colored region in the lower right of the plot shows where the test particle is trapped by the domain wall and its position oscillates, but the details of these oscillations are not captured at this resolution. The white dotted line shows where $\mu/\lambda^{1/3} = \text{MeV}$. Close to this line, domain walls can make up a fraction of the dark matter in the Universe today [36]. The white dash-dotted line corresponds to $d = 8.2 \times 10^{-5}$ m where quantum corrections from the scalar field could play the role of the cosmological constant [37,38].

that, at the lower end of this density range, the critical density is higher than the gas density achieved in the highest quality vacuum chambers used experimentally today.

III. INFINITE DOMAIN WALLS

At low densities, the scalar potential (3) has two degenerate minima. This allows for the formation of domain walls; topological defects whose field profile smoothly interpolates between these two minima. Infinite, straight, static domain walls have the form

$$\phi(y) = \phi_0 \tanh(y/d), \tag{4}$$

where $d = \frac{\sqrt{2}}{\mu}$ is the width of the domain wall, and

$$\phi_0^2 = \frac{\mu^2}{\lambda}\left(1 - \frac{\rho_0}{\rho_\star}\right). \tag{5}$$

The possibility of detecting scalar domain walls through their impact on the trajectories of matter particles has been considered in cosmology [41], Solar System dynamics [42], and laboratory experiments [30]. The behavior of a test particle of unit mass moving perpendicularly through an infinite, straight domain wall is governed by the sign of the Hamiltonian [30],

$$H_y = \frac{\dot{y}^2}{2} + \frac{\phi^2(y) - \phi_0^2}{2M^2}. \tag{6}$$

[Note that, because we are assuming a test particle of unit mass, the Hamiltonian in Eq. (6) has dimensions of velocity squared.] The critical initial conditions, position $y_{\text{crit}}(t=0)$ and velocity $\dot{y}_{\text{crit}}(t=0)$, separating the two regimes of behavior satisfy

$$\cosh\left(\frac{y_{\text{crit}}(t=0)}{d}\right) = \frac{\phi_0}{\dot{y}_{\text{crit}}(t=0)M}. \tag{7}$$

We see two types of behavior for a test particle, with $y_0 = y(0)$ and $\dot{y}_0 = \dot{y}(0)$:

(i) If $a^2 = 1 + \phi_0^2/(2H_y M^2) > 0$, the particle passes through the domain wall and

$$\frac{\sinh(\frac{y(t)}{d})}{a} = \sinh\left(\frac{\sqrt{2H_y}t}{d} + \text{arcsinh}\left(\frac{\sinh(\frac{y_0}{d})}{a}\right)\right). \tag{8}$$

(ii) If $\alpha^2 = -[1 + \phi_0^2/(2H_y M^2)] > 0$, the particle gets trapped within the domain wall and

$$\frac{\sinh(\frac{y(t)}{d})}{\alpha} = \sin\left(\frac{\sqrt{-2H_y}t}{d} + \text{arcsin}\left(\frac{\sinh(\frac{y_0}{d})}{\alpha}\right)\right). \tag{9}$$

The perturbation Δy caused by a domain wall to the motion of a particle that would otherwise move at constant speed is shown in Fig. 1 for $\lambda = 10^{-10}$. Smaller (larger) values of λ give rise to stronger (weaker) fifth forces and larger (smaller) displacements.

IV. DETECTING DARK WALLS

We consider an idealized experiment inside a vacuum chamber whose walls have a fixed density and where the gas pressure (and density) inside the chamber can be varied. A necessary condition for domain walls to form is that the density of gas can be decreased with time through the critical density $\rho_\star = \mu^2 M^2$. We also require the density of the walls of the vacuum chamber to be above $\rho_\star$, so that the effective mass of the field inside the walls is large, and perturbations of the scalar field sourced outside the chamber are exponentially damped in the walls. We therefore require

$$\frac{5\times10^{-5}\rho_{\rm gas}}{10^{-18}\ {\rm g/cm^3}} < \left(\frac{M}{\rm GeV}\right)^2\left(\frac{\rm m}{d}\right)^2 < \frac{5\times10^{13}\rho_{\rm wall}}{\rm g/cm^3}, \tag{10}$$

where $\rho_{\rm gas}$ is the minimum value of the gas density inside the chamber. We also require that the width of the domain wall be smaller than the characteristic internal dimension of the vacuum chamber L; $d < L$.

We consider a spherical vacuum chamber with internal radius $L = 10$ cm. The density of the stainless steel walls of the chamber is $\rho_{\rm wall} = 8\ {\rm g/cm^3}$ and the minimum vacuum pressure is 10^{-11} mbar (corresponding to a vacuum gas density $\rho_{\rm gas} \approx 10^{-18}\ {\rm g/cm^3}$). The upper bounds on d and M/d required for domain walls to form are shown by the light opaque shaded regions in Fig. 1.

Deviations of the path of the test particle are detectable when $\Delta y \gtrsim 10\ \mu$m.[1] Systematic errors can be reduced with a differential measurement, for example, using a rotational flange to change the relative position of the test particles and the domain wall, so that the trajectories of particles that pass through a domain wall can be compared with those that do not. Uncertainties in the position can be reduced by a large (>1000) number of repeats.

A. Formation of domain walls

If the gas density inside the vacuum chamber is lowered uniformly through $\rho_\star$, then domain walls can form through the Kibble-Zurek mechanism [43–45]. Assuming that the gas density varies linearly with time such that $|\rho(t) - \rho_\star|/\rho_\star = t/T$, for some characteristic timescale T, then we expect that domain walls will start to form at time $\hat{t} \approx (T/\mu^2)^{1/3}$ (when evolution of the scalar field is no longer adiabatic) and with correlation length $L_c = d(T/2d)^{1/3}$. If the correlation length is smaller than the characteristic size of the vacuum chamber, $L_c < L$, then domain walls may form inside the chamber. This requires (reintroducing physical units)

$$\left(\frac{d}{\rm m}\right)^2 \lesssim 10^{-12}\left(\frac{L}{\rm m}\right)^3\frac{\rm sec}{T}. \tag{11}$$

The timescale for lowering the gas density of a vacuum chamber varies. If, for example, $T = 10^{-1}$ s, then domain walls with $d \lesssim 2.7\times10^{-5}$ m will have a correlation length smaller than the size of the vacuum chamber, 0.1 m. From Fig. 1 we see that there is little parameter space available for such thin domain walls to form in our idealized experiment. Thicker domain walls will be unlikely to form inside the spherical chamber through the Kibble-Zurek mechanism alone.

[1]Test particle positions can be imaged with a high-precision camera, for example Princeton Instruments PIXIS 1024 BR back-illuminated CCD camera or the iXon Ultra 888 EMCCD. Both cameras have imaging resolution < 1 μm.

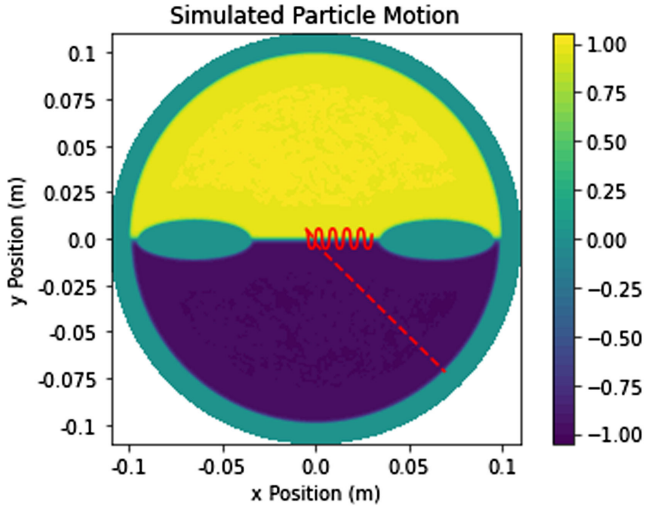

FIG. 3. The motion of particles with initial position $\mathbf{x}_0 = (-0.005, 0.005)$ m and initial velocities $\dot{\mathbf{x}}_0 = (0.001, -0.001)$ m/s (solid line) and $(0.01, -0.01)$ m/s (dashed line). Scalar parameters are $\mu = 2.0\times10^{-13}$ GeV, $M = 100$ GeV, and $\lambda = 10^{-10}$ (lower black dot in Fig. 1). The color bar indicates the value of the scalar field, with ϕ_0 normalized to 1. The simulation runs for $t = 35$ s.

The Kibble mechanism describes the formation of domain walls in infinite space. In a finite sized vacuum chamber, structures inside the chamber can both encourage domain walls to form and influence where they form. If spikes protrude from the walls of the chamber, such that the space between the tips of the spikes is smaller than, or similar to, the Compton wavelength d of the scalar field, then the field will not have space to change its value from zero, even as the density of the chamber is lowered. It has been shown previously [26,27,30] that matter structures with even larger separations can be used to stabilize domain walls and pin them in place. As a result, the presence of spikes protruding from the walls of a vacuum chamber make it extremely likely that a nontrivial scalar field profile is present.[2] An example of such a configuration is shown in Fig. 3, assuming rotational symmetry around the y axis. Simulation of the time-dependent behavior of the field during the formation of the domain walls is left for future work.

To further encourage a domain wall to form, a shutter may be placed in the narrow waist between the spikes. While the density of the vacuum gas is lowered, the shutter is closed, allowing the field to evolve separately on either side. In each region, the field has an equal chance of rolling to either of the two minima of Eq. (5) as the density of the vacuum gas decreases. Once the vacuum chamber is fully pumped out, the shutter is opened quickly. In the event that the field has rolled to a different minimum in each region, in

[2]The field may not choose different vacua on either side of the spikes. So the experiment would need to be repeated multiple times to increase the probability that a domain wall forms.

the vicinity of the spikes the field will interpolate between those two values, describing a domain wall. If the shutter is of similar width to or thinner than the domain wall width, we do not expect it to experience any friction when opening, as the field profile will have the same form before the shutter opens (due to the presence of the shutter) and after (due to the presence of the domain wall). If the shutter is thicker than the domain wall, it may experience some friction, but, for the parameters we study in this work, we expect this to be sufficiently small that it would not affect the operation of the shutter.

B. Observable signatures of domain walls

We consider the effects of a domain wall on the motion of a test particle falling freely through the wall. After the period of formation we expect any scalar oscillations to be radiated away and the domain wall to be static. To determine this profile we use a code adapted from SELCIE [46], which can solve static, nonlinear scalar field equations around arbitrary-shaped matter configurations. We solve for the motion of a test particle in this background using a leapfrog algorithm. These codes are described in the Supplemental Material [47].

We consider two example cases, a thin and a thick domain wall, which correspond to two currently unconstrained points in parameter space, indicated in Fig. 1. The model parameters are chosen to illustrate both the robustness of our numerical codes and that detection of domain walls is within the sensitivity of current technology. For both scenarios we keep the geometry of the chamber fixed.

1. Thin domain walls

A thin domain wall is one where the width of the domain wall is much smaller than the internal dimensions of the vacuum chamber. As an example, we use $\mu = 2.0 \times 10^{-13}$ GeV, $M = 100$ GeV, and $\lambda = 10^{-10}$.

A particle starts at $y_0 = 5 \times 10^{-3}$ m above the center of the domain wall. The analytic estimate in Eq. (7) indicates that particles with initial velocities below $\dot{y}_0 = 3 \times 10^{-2}$ m/s will be trapped by the domain wall, and those with higher initial velocities will pass through the wall. This agrees with the results of our numerical simulations, shown in Fig. 3, where we show trajectories for particles with initial velocities $\dot{y}_0 = 10^{-3}$ and $\dot{y}_0 = 10^{-2}$ m/s. Such small initial velocities can be achieved experimentally; see, for example, Ref. [48].

This example allows us to check the validity of the analytic approximation of Eq. (7) by comparing the horizontal and vertical motions of the trapped particle. If the initial horizontal position and velocity are $x_0 = -5 \times 10^{-3}$ m and $\dot{x}_0 = 10^{-3}$ m/s, the particle will have position $x = +5 \times 10^{-3}$ m/s after 10 s. Numerical evolution reproduces this motion with a relative error of 0.04%. In contrast, the domain wall causes an acceleration in the vertical direction. After 10 s, the analytic calculation predicts that the position of the particle is $y = -5.78 \times 10^{-3}$ m, while our numerical integration finds a position of $y = -5.30 \times 10^{-3}$ m, a difference of 8%. So even when the domain wall is thin compared to the size of the chamber, the experimental environment needs to be simulated in order to produce an accurate prediction of the motion of test particles.

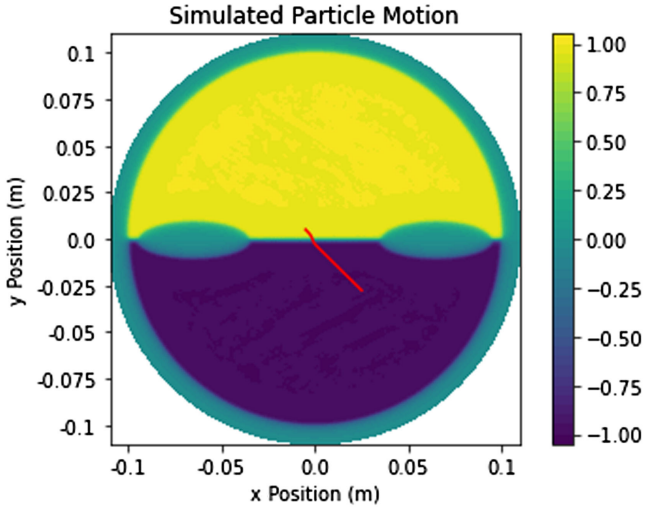

FIG. 4. The motion of a particle with initial position $\mathbf{x}_0 = (-0.005, 0.005)$ m and initial velocity $\dot{\mathbf{x}}_0 = (10^{-5}, -10^{-5})$ m/s. Scalar parameters are $\mu = 2.0 \times 10^{-14}$ GeV, $M = 10^4$ GeV, and $\lambda = 10^{-10}$ (upper black dot in Fig. 1). The color bar indicates the value of the scalar field, with ϕ_0 normalized to 1. The simulation runs for $t = 3000$ s.

2. Thick domain walls

We do not expect thick domain walls, with width comparable to the internal dimensions of the vacuum chamber, to be well modeled by the analytic approximation of an infinite straight domain wall. As an example, we use $\mu = 2.0 \times 10^{-14}$ GeV, $M = 10^4$ GeV, and $\lambda = 10^{-10}$. For values of the initial velocity down to 10^{-5} m/s, we find that the particle always passes through the wall. An example trajectory can be seen in Fig. 4.

For a particle starting at a point $y_0 = 5 \times 10^{-3}$ m we find that, at the accuracy of our simulation, the effects of the domain wall are only visible for initial velocities $\dot{y}_0 = 10^{-5}$ m/s or lower. For such a particle, we find that after a period of 10^3 s the particle's position is $y = -7.7 \times 10^{-3}$ m, whereas with no domain wall, the particle's position would be $y = -5 \times 10^{-3}$ m. The analytic prediction predicts the position at this time to be $y = -1.2 \times 10^{-3}$ m, a difference that would be detectable with a high-resolution camera.

V. CONCLUSION

Light scalar fields can form part or all of the dark matter and dark energy needed to complete our cosmological model. Domain walls are a signature of scalar fields with

symmetry breaking potentials. When the scalar field couples to matter, test particles passing through a domain wall will experience a fifth force. When velocities are low, the particles are trapped within the potential well of the domain wall, and when velocities are larger, the trajectory of the particle is deflected by the domain wall.

In this work we have argued that structures inside an experimental vacuum chamber, produced, for example, by 3D printing [49], can be exploited to pin domain walls in place in order to allow their impact on the motion of a test particle to be detected. In the absence of the structures, the domain walls are unlikely to form or will be short-lived. These structures mean it is necessary to solve for the scalar field profile numerically, which we demonstrate for a selection of model parameters. Although we have assumed a spherical vacuum chamber with protruding spikes, we expect this to generalize to realistic experiments as the key feature is just that there are two vacuum regions, larger than the Compton wavelength of the scalar field, within which the field can reach its minimum value. For an example choice of $\lambda = 10^{-10}$, we investigated whether the approximation of an infinite straight domain wall holds inside the vacuum chamber, finding that, when the width of the domain wall is a tenth of the internal dimension of the vacuum chamber, taking into account the vacuum chamber structure, including the spikes, leads to a change in the predicted position of the particle by an order one factor.

We find that, across a range of currently unconstrained parameter space, domain walls can give rise to observable deflections in particle motion, including the trapping of test particles within the domain wall. Figures 1 and 2 show that a first generation experiment with sensitivity of the position of the test particles will have access to significant regions of the model parameter space, including, for $\lambda = 10^{-30}$, parts of parameter space where the domain walls could make up part of the dark matter or cosmological constant in the Universe. For smaller values of λ, the fifth force increases, meaning that such an experiment could also be sensitive to parts of parameter space where domain walls could source the stochastic gravitational-wave background; however, we acknowledge that such values may be considered unnatural or fine-tuned.

This opens up exciting possibilities for relatively simple experiments with cold atoms or molecules to detect or constrain this beyond the Standard Model physics.

The source code, plotting scripts, and scalar field solutions can be made available on reasonable request to the authors.

ACKNOWLEDGMENTS

C. B. is supported by a Research Leadership Award from the Leverhulme Trust and STFC Grant No. ST/T000732/1. L. H. and M. F. acknowledge support by Innovate UK Projects No. 133086 and No. 10031462, the EPSRC Grants No. EP/R024111/1, No. EP/T001046/1, No. EP/Y005139/1, and the JTF Grant No. 62420.

[1] W. Hu, R. Barkana, and A. Gruzinov, Phys. Rev. Lett. **85**, 1158 (2000).
[2] E. G. M. Ferreira, Astron. Astrophys. Rev. **29**, 7 (2021).
[3] E. J. Copeland, M. Sami, and S. Tsujikawa, Int. J. Mod. Phys. D **15**, 1753 (2006).
[4] A. Joyce, B. Jain, J. Khoury, and M. Trodden, Phys. Rep. **568**, 1 (2015).
[5] T. Clifton, P. G. Ferreira, A. Padilla, and C. Skordis, Phys. Rep. **513**, 1 (2012).
[6] T. Damour, F. Piazza, and G. Veneziano, Phys. Rev. D **66**, 046007 (2002).
[7] M. Gasperini, F. Piazza, and G. Veneziano, Phys. Rev. D **65**, 023508 (2001).
[8] T. Binoth and J. J. van der Bij, Z. Phys. C **75**, 17 (1997).
[9] B. Patt and F. Wilczek, arXiv:hep-ph/0605188.
[10] R. M. Schabinger and J. D. Wells, Phys. Rev. D **72**, 093007 (2005).
[11] C. Englert, T. Plehn, D. Zerwas, and P. M. Zerwas, Phys. Lett. B **703**, 298 (2011).
[12] M. Bauer, P. Foldenauer, P. Reimitz, and T. Plehn, SciPost Phys. **10**, 030 (2021).
[13] J. Beacham *et al.*, J. Phys. G **47**, 010501 (2020).
[14] A. Slosar *et al.*, arXiv:1903.12016.
[15] P. Brax, S. Casas, H. Desmond, and B. Elder, Universe **8**, 11 (2021).
[16] K. Hinterbichler and J. Khoury, Phys. Rev. Lett. **104**, 231301 (2010).
[17] K. Hinterbichler, J. Khoury, A. Levy, and A. Matas, Phys. Rev. D **84**, 103521 (2011).
[18] D. F. Mota and D. J. Shaw, Phys. Rev. D **75**, 063501 (2007).
[19] H. Dehnen, H. Frommert, and F. Ghaboussi, Int. J. Theor. Phys. **31**, 109 (1992).
[20] E. Gessner, Astrophys. Space Sci. **196**, 29 (1992).
[21] T. Damour and A. M. Polyakov, Nucl. Phys. **B423**, 532 (1994).
[22] M. Pietroni, Phys. Rev. D **72**, 043535 (2005).
[23] K. A. Olive and M. Pospelov, Phys. Rev. D **77**, 043524 (2008).
[24] A. Vilenkin, Phys. Rep. **121**, 263 (1985).
[25] A. Lazanu, C. J. A. P. Martins, and E. P. S. Shellard, Phys. Lett. B **747**, 426 (2015).
[26] C. Llinares and L. Pogosian, Phys. Rev. D **90**, 124041 (2014).

[27] J. A. Pearson, Phys. Rev. D **90**, 125011 (2014); **91**, 049901(A) (2015).
[28] O. Christiansen, F. Hassani, M. Jalilvand, and D. F. Mota, J. Cosmol. Astropart. Phys. 05 (2020) 009.
[29] A. P. Naik and C. Burrage, J. Cosmol. Astropart. Phys. 08 (2022) 020.
[30] C. Llinares and P. Brax, Phys. Rev. Lett. **122**, 091102 (2019).
[31] B. Nosrati and N. Khosravi, Phys. Rev. D **108**, 083511 (2023).
[32] K. Nakayama, F. Takahashi, and N. Yokozaki, Phys. Lett. B **770**, 500 (2017), https://www.sciencedirect.com/science/article/pii/S037026931730360X?via%3Dihub.
[33] K. Saikawa, Universe **3**, 40 (2017).
[34] R. Z. Ferreira, A. Notari, O. Pujolas, and F. Rompineve, J. Cosmol. Astropart. Phys. 02 (2023) 001.
[35] E. Babichev, D. Gorbunov, S. Ramazanov, R. Samanta, and A. Vikman, Phys. Rev. D **108**, 123529 (2023).
[36] Y. V. Stadnik, Phys. Rev. D **102**, 115016 (2020).
[37] P. Brax, A. C. Davis, and B. Elder, Phys. Rev. D **106**, 044040 (2022).
[38] A. Upadhye, W. Hu, and J. Khoury, Phys. Rev. Lett. **109**, 041301 (2012).
[39] T. Jenke, J. Bosina, J. Micko, M. Pitschmann, R. Sedmik, and H. Abele, Eur. Phys. J. Special Topics **230**, 1131 (2021).
[40] D. O. Sabulsky, I. Dutta, E. A. Hinds, B. Elder, C. Burrage, and E. J. Copeland, Phys. Rev. Lett. **123**, 061102 (2019).
[41] A. Vilenkin and E. P. S. Shellard, *Cosmic Strings and Other Topological Defects* (Cambridge University Press, Cambridge, England, 2000), ISBN 978-0-521-65476-0.
[42] D.-C. Dai, D. Minic, and D. Stojkovic, J. High Energy Phys. 03 (2022) 207.
[43] T. W. B. Kibble, J. Phys. A **9**, 1387 (1976).
[44] W. H. Zurek, Nature (London) **317**, 505 (1985).
[45] W. H. Zurek, Phys. Rep. **276**, 177 (1996).
[46] C. Briddon, C. Burrage, A. Moss, and A. Tamosiunas, J. Cosmol. Astropart. Phys. 12 (2021) 043.
[47] See Supplemental Material at http://link.aps.org/supplemental/10.1103/PhysRevD.109.123023 for a description of the numerical codes used to compute the scalar field profile and the motion of a test particle on this background.
[48] T. A. Pasquini, Y. Shin, C. Sanner, M. Saba, A. Schirotzek, D. E. Pritchard, and W. Ketterle, Phys. Rev. Lett. **93**, 223201 (2004).
[49] N. Cooper, L. Coles, S. Everton, I. Maskery, R. Campion, S. Madkhaly, C. Morley, J. O'Shea, W. Evans, R. Saint *et al.*, Addit. Manuf. **40**, 101898 (2021).